Neutrino signal of electron-capture supernovae from core collapse to cooling

L. Hüdepohl,[1] B. Müller,[1] H.-T. Janka,[1] A. Marek,[1] and G. G. Raffelt[2]

[1] *Max-Planck-Institut für Astrophysik, Karl-Schwarzschild-Str. 1, D-85748 Garching, Germany*
[2] *Max-Planck-Institut für Physik, Werner-Heisenberg-Institut, Föhringer Ring 6, D-80802 München, Germany*

(Dated: July 22, 2010)

An $8.8\,M_\odot$ electron-capture supernova (SN) was simulated in spherical symmetry consistently from collapse through explosion to nearly complete deleptonization of the forming neutron star. The evolution time of about 9 s is short because of nucleon-nucleon correlations in the neutrino opacities. After a brief phase of accretion-enhanced luminosities ($\sim$200 ms), luminosity equipartition among all species becomes almost perfect and the spectra of $\bar\nu_e$ and $\bar\nu_{\mu,\tau}$ very similar. We discuss consequences for the neutrino-driven wind as a nucleosynthesis site and for flavor oscillations of SN neutrinos.

PACS numbers: 97.60.Bw, 95.85.Ry, 26.30.-k, 97.60.Jd

Introduction.—During the first seconds after collapse, a supernova (SN) core emits its binding energy, roughly 10% of its rest mass, in the form of neutrinos. In the delayed explosion paradigm, supported at least for some progenitor stars by recent simulations [1], neutrinos revive the stalled shock wave and by their energy deposition explode the star [2]. Later they drive a powerful wind and through β-processes determine its role as a possible site for r-process nucleosynthesis [3]. Inevitable deviations from spherical symmetry allow the neutrino flux to emit gravitational waves [4] and to impart a potentially large neutron-star recoil [5].

A sparse neutrino signal was observed from SN 1987A. Existing and foreseen large detectors [6] will operate for decades, suggesting the next galactic SN will provide a high-statistics signal and allow for a direct glance of its inner workings. The cosmic diffuse neutrino background from all past SNe (DSNB) is almost certainly detectable if gadolinium loading of Super-Kamiokande succeeds [7] or by future large scintillator detectors [8], pushing the frontiers of neutrino astronomy to cosmic distances.

The fluxes and spectra differ for the species ν_e, $\bar\nu_e$ and ν_x (representing any of $\nu_{\mu,\tau}$ or $\bar\nu_{\mu,\tau}$). Flavor oscillations swap $\nu_e \leftrightarrow \nu_x$ and $\bar\nu_e \leftrightarrow \bar\nu_x$ in part or completely, a process strongly affected by collective effects and Mikheev-Smirnov-Wolfenstein resonances [9]. What is seen in the neutrino-driven wind or by a detector thus depends not only on what is emitted, but also on the matter profile and neutrino mixing parameters.

Quantitative studies in these areas are impeded by large uncertainties of the expected fluxes and spectra. This problem partly derives from uncertainties of the explosion mechanism itself and input physics such as the nuclear equation of state (EoS). Significant variations are expected in dependence of the progenitor mass, and sometimes rotation and magnetic fields may come into play. However, even without such complications, the range of predictions is large for the post-explosion cooling phase when by far most of the neutrino loss happens.

The pioneering work of the Livermore group combined relativistic hydrodynamics with multi-group three-flavor neutrino diffusion in spherical symmetry (1D), simulating the entire evolution self-consistently [10]. The spectra were hard over a period of at least 10 s with increasing hierarchy $\langle\epsilon_{\nu_x}\rangle > \langle\epsilon_{\bar\nu_e}\rangle > \langle\epsilon_{\nu_e}\rangle$. These models, however, included significant numerical approximations and omitted neutrino reactions that were later recognized to be important [11]. A crucial ingredient to enhance the early neutrino fluxes was a neutron-finger mixing instability, which today is disfavored [12].

Relativistic calculations of proto neutron star (PNS) cooling with a flux-limited equilibrium [13, 14] or multi-group diffusion treatment [15] found monotonically decreasing neutrino energies after no more than a short ($\lesssim 100$ ms) period of increase. Pons et al. [16] studied PNS cooling for different EoS and masses, using flux-limited equilibrium transport with diffusion coefficients adapted to the underlying EoS. They always found spectral hardening over 2–5 s before turning over to cooling.

New opportunities to study the neutrino signal consistently from collapse to late-time cooling arise from the class of "electron-capture SNe" or "O-Ne-Mg core SNe." These low-mass (8–10 $M_\odot$) stars collapse because of rapid electron capture on neon and magnesium and could represent up to 30% of all SNe [17]. They are the only cases where 1D simulations obtain neutrino-powered explosions [18] and 2D yields only minor dynamical and energetic modifications [19]. Therefore, it is conceivable to carry hydrodynamic simulations with modern neutrino Boltzmann solvers in 1D all the way to PNS cooling.

Very recently, the Basel group has circulated first results of the PNS evolution [20] for a representative $8.8\,M_\odot$ progenitor [21] using Shen et al.'s EoS [22], which is relatively stiff and yields cold NS radii around 15 km.

Here we report our own long-term simulations of the same progenitor and the same EoS, facilitating a direct comparison. (Our results with different choices of EoS will be reported elsewhere.) However, we explore different neutrino interaction rates, leading to significant differences that we will discuss.

Numerical method.—Our simulations were performed with the Prometheus/Vertex code. It couples an ex-

plicit third-order Riemann-solver-based Newtonian hydrodynamics code with an implicit multi-flavor, multi-energy-group two-moment closure scheme for neutrino transport. The variable Eddington-factor closure is obtained from a model Boltzmann equation [23]. We account for general relativistic (GR) corrections with an effective gravitational potential (case A of Ref. [24]) and the transport includes GR redshift and time dilation. Tests showed good overall agreement until several 100 ms after core bounce [24, 25] with fully relativistic simulations of the Basel group's AGILE-BOLTZTRAN code. A more recent comparison with a GR program [26] that combines the COCONUT hydro solver [27] with the VERTEX neutrino transport, reveals almost perfect agreement except for a few quantities with deviations of at most 7–10% until several seconds. The total neutrino loss of the PNS agrees with the relativistic binding energy of the NS to roughly 1%, defining the accuracy of global energy and lepton-number conservation in our simulations.

Our primary case (Model Sf) includes the full set of neutrino reactions described in Appendix A of Ref. [28] with the original sources. In particular, we account for nucleon recoils and thermal motions, nucleon-nucleon (NN) correlations, weak magnetism, a reduced effective nucleon mass and quenching of the axial-vector coupling at high densities, NN bremsstrahlung, $\nu\nu$ scattering, and $\nu_e\bar{\nu}_e \to \nu_{\mu,\tau}\bar{\nu}_{\mu,\tau}$. In addition, we include electron capture and inelastic neutrino scattering on nuclei [29].

To compare with previous simulations and the Basel work [20] we also consider a reduced set of opacities [30], omitting pure neutrino interactions, recoils in neutrino-nucleon interactions, and NN correlations (Model Sr). This case closely resembles the Basel results.

Long-term simulations.—In Fig. 1 we show the evolution of the ν_e, $\bar{\nu}_e$ and ν_x luminosities and of the average energies, defined as the ratio of energy to number fluxes. The dynamical evolution, development of the explosion, and shock propagation were previously described [18, 19]. The characteristic phases of neutrino emission are clearly visible: (i) Luminosity rise during collapse. (ii) Shock breakout burst. (iii) Accretion phase, ending already at $\sim$0.2 s post bounce when neutrino heating reverses the infall. (iv) Kelvin-Helmholtz cooling of the hot PNS with a duration of 10 s or more, accompanied by mass outflow in the neutrino-driven wind.

The PNS evolves in the familiar way [13, 16] through deleptonization and energy loss. It contracts, initially heating up by compression and down-scattering of energetic ν_e produced in captures of highly degenerate electrons. With progressing neutronization the PNS cools, approaching a state of β-equilibrium with vanishing ν_e chemical potential μ_{ν_e} and minimal electron content.

In Model Sf, deleptonization and cooling take $\sim$10 s until ν transparency is approached. For $t > 8.9$ s we find $T \lesssim 6$ MeV and $\mu_{\nu_e} \sim 0$ throughout, and $\dot{N}_{\rm L} \ll 10^{53}\,{\rm s}^{-1}$. The final baryon mass is $M_{\rm b} = 1.366\,M_\odot$ with radius

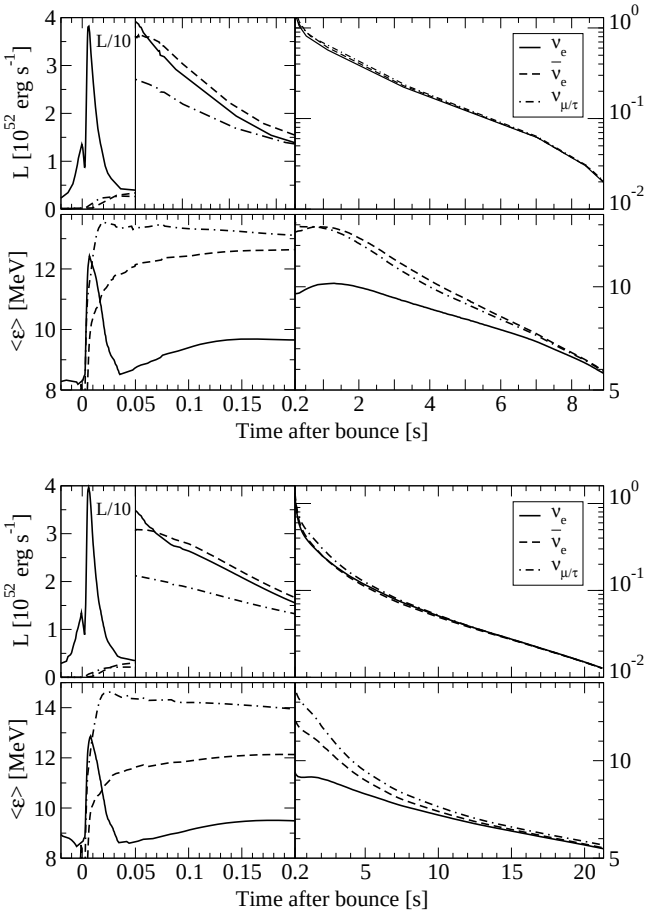

FIG. 1: Neutrino luminosities and mean energies observed at infinity. *Top:* Full set of neutrino opacities (Model Sf). *Bottom:* Reduced set (Model Sr).

$\sim$15 km. Neutrinos have carried away lepton number of 6.57×10^{56} and energy $E_\nu = 1.66\times10^{53}$ erg, so the gravitational mass is $M = M_{\rm b} - E_\nu/c^2 = 1.273\,M_\odot$. The evolution is faster than in previous simulations [16] or in Model Sr because of opacity suppression by nucleon correlations at high density [31]. In Model Sr, deleptonization remains incomplete at 21 s when $\dot{N}_{\rm L} \sim 2\times10^{53}\,{\rm s}^{-1}$, $T \sim 17$ MeV in the center, and only 96% of the gravitational binding energy have been lost.

Differences are also conspicuous in the luminosities. Until 5.5 s they are higher (up to 60% at $t \sim 2$ s) in Model Sf, whereas afterwards they drop much faster compared to Model Sr. On the other hand, for $t \gtrsim 0.2$ s, after the end of accretion, the luminosities in both models become independent of flavor within 10% or better. The total radiated E_ν shows nearly equipartition: 20% are carried away by ν_e, 16% by $\bar{\nu}_e$, and 4×16% by ν_x.

Spectra.—The mean neutrino energies evolve very differently in the two cases. While they increase over 1–1.5 s for ν_e and $\bar{\nu}_e$ in Model Sf, this phase lasts only until $\sim$0.2 s in Model Sr. The opacities are lower and thus the neutrino spheres at higher T, so Model Sf has larger $\langle\epsilon_{\nu_e}\rangle$ and

$\langle\epsilon_{\bar\nu_e}\rangle$ for several seconds before dropping below Model Sr due to the faster overall evolution.

The canonical spectral hierarchy $\langle\epsilon_{\nu_x}\rangle > \langle\epsilon_{\bar\nu_e}\rangle > \langle\epsilon_{\nu_e}\rangle$ persists in Model Sr during the cooling phase, while in Model Sf we find $\langle\epsilon_{\nu_x}\rangle \approx \langle\epsilon_{\bar\nu_e}\rangle > \langle\epsilon_{\nu_e}\rangle$ and actually $\langle\epsilon_{\nu_x}\rangle$ and $\langle\epsilon_{\bar\nu_e}\rangle$ slightly cross over. The close similarity of $\langle\epsilon_{\nu_x}\rangle$ and $\langle\epsilon_{\bar\nu_e}\rangle$ was previously found [11] as a consequence of recoil in $\nu_x N \to N\nu_x$, suppressing the high-energy ν_x tail (spectral pinching) and reducing $\langle\epsilon_{\nu_x}\rangle$.

A quasi-thermal spectrum can be characterized by its lowest energy moments $\bar\epsilon \equiv \langle\epsilon_\nu\rangle$ and $\langle\epsilon_\nu^2\rangle$. Simple analytic fits use a nominal Fermi-Dirac (FD) distribution with temperature T and degeneracy parameter η [32] or a modified power law $f_\alpha(\epsilon) = (\epsilon/\bar\epsilon)^\alpha \mathrm{e}^{-(\alpha+1)\epsilon/\bar\epsilon}$ [11]. The spectrum is "pinched" (narrower than a thermal FD) if $p = a^{-1}\langle\epsilon_\nu^2\rangle/\langle\epsilon_\nu\rangle^2 = a^{-1}(2+\alpha)/(1+\alpha) < 1$ where $a \approx 1.3029$. So it is pinched for $p < 1$, $\eta > 0$ and $\alpha \gtrsim 2.3$ and anti-pinched otherwise. A Maxwell-Boltzmann (MB) spectrum has $\alpha = 2$, $\eta = -\infty$ and $p \approx 1.0234$.

In Model Sf the ν_e spectrum is always pinched, while $\bar\nu_e$ and ν_x are mildly anti-pinched ($-1 < \eta < 0$) for $3\,\mathrm{s} \lesssim t \lesssim 7\,\mathrm{s}$ (Fig. 2). At the end of the simulation $\langle\epsilon\rangle$ becomes almost identical for all species. The same applies to the spectral shape, which approaches a thermal FD function ($\alpha \approx 2.5$, $p \approx 0.99$, $\eta \approx 0.6$).

The time-integrated spectra of the number fluxes have $\langle\epsilon_{\nu_e,\bar\nu_e,\nu_x}\rangle = 9.40$, 11.44, and 11.44 MeV. The spectrum is moderately pinched for ν_e ($p \approx 0.96$, $\alpha \approx 3.0$, $\eta \approx 1.7$), a nearly thermal FD for $\bar\nu_e$ ($p \approx 0.99$), and slightly anti-pinched for ν_x ($p \approx 1.017$, $\alpha \approx 2.1$, $\eta \approx -1.5$).

Effective radiating surface.—The neutrino luminosities L_ν and effective temperatures T_e can be used to estimate the NS circumferential radius R. (This does not apply to late-time volume emission and the early accretion-powered phase.) The Stefan-Boltzmann law is $L_\nu = 4\pi\phi\sigma_\nu T_\mathrm{e}^4 R_\infty^2$ in terms of quantities measured at infinity and $\sigma_\nu = 4.751\times10^{35}\,\mathrm{erg\,MeV^{-4}\,cm^{-2}\,s^{-1}}$ if T_e is measured in MeV. A MB spectrum is assumed ($T_\mathrm{e} = \frac{1}{3}\langle\epsilon_\nu\rangle$) with isotropic emission at the radiating surface. All deviations from these assumptions are absorbed in a "grayness factor" ϕ.

We define R as the location where $\rho = 10^{11}\ \mathrm{g\,cm^{-3}}$. GR corrections imply that $R_\infty = R/\sqrt{1-2\beta}$ where $\beta = GM/(Rc^2)$ and M is the PNS gravitational mass. In Model Sf, R/R_∞ drops from an initial value near 1 to 0.88 at 3 s, followed by a slow decline to 0.87 at 8 s. M is linked to the gravitational binding energy and thus to the total ν energy release by $E_\nu \approx 0.6\beta Mc^2(1-0.5\beta)^{-1}$ [33], reproduced very well in our simulations. We propose to use these relations with measured values of E_ν, $\langle\epsilon_{\bar\nu_e}\rangle$ and $L_{\bar\nu_e}$ during the cooling phase to determine M and R from the signal of a future galactic SN.

The grayness factors for Model Sf are shown in Fig. 2. Their time variation is considerable, but we found $\phi \approx 0.6$ to be a good choice for $\bar\nu_e$ around the time (5–6 s) of the $\alpha(t)$ minimum. This estimate applies for different

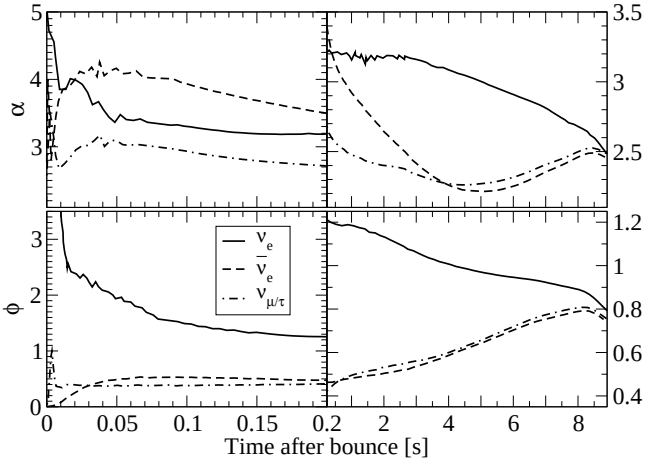

FIG. 2: Spectral fit parameter α and luminosity grayness factor ϕ for Model Sf.

EoS that we have tested. We always found very similar evolutions $\alpha(t)$ and $\phi(t)$.

Neutrino-driven wind.—Absorption of ν_e and $\bar\nu_e$ on nucleons determines the n/p ratio $Y_e^{-1} - 1$ in the neutrino-driven wind [3], where Y_e is the electron/baryon ratio. R-process nucleosynthesis conditions depend on n/p in addition to the entropy per baryon s, the expansion timescale τ_exp (between $T = 0.5\,\mathrm{MeV}$ and $0.5/e\,\mathrm{MeV}$), and the mass-loss rate $\dot M$, which in turn depend on the neutrino energy deposition [3].

Since $\langle\epsilon_{\nu_e}\rangle$ and $\langle\epsilon_{\bar\nu_e}\rangle$ are very similar and because $\bar\nu_e$ absorptions are impeded by the n/p mass difference, one finds Y_e values significantly above 0.5 [20]. We confirm this result in our Model Sf (Fig. 3). The mean energies approach each other at late times, so Y_e grows monotonically and reaches 0.63 after 9 s. This excludes the wind in electron-capture SNe as a site of r-processing. Flavor conversions of active neutrinos cannot change this conclusion because $\langle\epsilon_{\bar\nu_e}\rangle \sim \langle\epsilon_{\bar\nu_x}\rangle$.

Conclusions.—Our simulations of an electron-capture

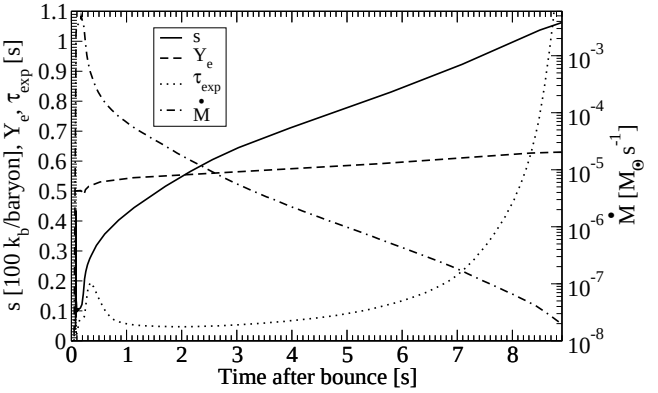

FIG. 3: Neutrino-driven wind properties (Model Sf). The expansion time scale τ_exp refers to the T-decline at 0.5 MeV.

SN reveal important features of the neutrino signal, especially for the cooling phase. We confirm that $\langle\epsilon_{\bar{\nu}_e}\rangle$ and $\langle\epsilon_{\nu_e}\rangle$ are too similar to support r-process conditions [20]. Moreover, we find $\langle\epsilon_{\nu_x}\rangle \approx \langle\epsilon_{\bar{\nu}_e}\rangle > \langle\epsilon_{\nu_e}\rangle$, implying that flavor conversions in the $\bar{\nu}$ sector would have hardly any impact. It was recognized previously that the exact relation between $\langle\epsilon_{\nu_x}\rangle$ and $\langle\epsilon_{\bar{\nu}_e}\rangle$ depends on fine points of the neutrino interaction rates [11]. The mild hierarchy $\langle\epsilon_{\nu_x}\rangle > \langle\epsilon_{\bar{\nu}_e}\rangle$ in our Model Sr is caused by the omission of nucleon recoils in $\nu_x N \to N\nu_x$.

Our runs for electron-capture SNe with other EoS yield similar results. The PNS cooling phase is comparable for all SNe and our conclusions probably carry over to more massive stars. In fact, the Basel group considered artificially triggered explosions of higher-mass SNe and found similar ν emission properties as in their electron-capture case.

It is surprising that luminosity equipartition among species during the cooling phase is almost perfect in our simulations as well as the Basel and Livermore ones, despite very different treatments of neutrino transport and different spectral hierarchies.

During accretion-powered neutrino emission, $L_{\nu_e,\bar{\nu}_e}$ is significantly larger than L_{ν_x} in all simulations as physically expected, and flavor oscillations could well show up in a high-statistics SN $\bar{\nu}_e$ signal. Differences between the ν_e and ν_x fluxes and spectra are pronounced in all phases. Therefore, a large ν_e detector would be especially useful.

Our time-integrated $\langle\epsilon_{\bar{\nu}_e,\bar{\nu}_x}\rangle = 11.4$ MeV is relatively low, for other EoS only $\sim$0.5 MeV higher, and also similar to the Basel simulations with different progenitor masses. Taking $\langle\epsilon_{\bar{\nu}_e,\bar{\nu}_x}\rangle = 11$–$12$ MeV as a typical range, the agreement with SN1987A data is much better than had been thought previously [35].

To confirm our findings one should study more models with different masses and EoS and further improve the neutrino-matter interactions. Moreover, PNS convection should be investigated because it can modify some ν flux quantities by 10–30% during accretion [36] and could cause larger differences later [37]. All of these effects may influence the flavor hierarchy and absolute $\langle\epsilon\rangle$ scale. Also light clusters (deuterons, tritons, helium-3) in the surface medium of the PNS could modify the wind composition [38]. However it seems unlikely that Y_e would reduce to $\sim$0.2 as required for a strong r-process [34], given the s and $\tau_{\rm exp}$ values of our models.

We acknowlege partial support by DFG grants No. SFB/TR 7, SFB/TR 27, EXC 153 and computer time at the HLRS in Stuttgart.

[1] H.-T. Janka *et al.*, Phys. Rept. **442**, 38 (2007).
[2] H. A. Bethe and J. R. Wilson, Astrophys. J. **295**, 14 (1985).
[3] Y.-Z. Qian and S. E. Woosley, Astrophys. J. **471**, 331 (1996).
[4] R. Epstein, Astrophys. J. **223**, 1037 (1978).
[5] D. Lai, D. F. Chernoff and J. M. Cordes, Astrophys. J. **549**, 1111 (2001). G. M. Fuller *et al.*, Phys. Rev. D **68**, 103002 (2003).
[6] K. Scholberg, Proc. Neutrino 2006, astro-ph/0701081.
[7] H. Watanabe *et al.* [Super-Kamiokande Collaboration], Astropart. Phys. **31**, 320 (2009).
[8] D. Autiero *et al.*, JCAP **0711**, 011 (2007).
[9] A. Dighe, J. Phys. Conf. Ser. **136**, 022041 (2008).
[10] T. Totani *et al.*, Astrophys. J. **496**, 216 (1998). H. E. Dalhed, J. R. Wilson and R. W. Mayle, Nucl. Phys. Proc. Suppl. **77**, 429 (1999).
[11] M. T. Keil, G. G. Raffelt and H.-T. Janka, Astrophys. J. **590**, 971 (2003).
[12] S. W. Bruenn and T. Dineva, Astrophys. J. **458**, L71 (1996).
[13] A. Burrows and J. M. Lattimer, Astrophys. J. **307**, 178 (1986).
[14] W. Keil and H.-T. Janka, Astron. Astrophys. **296**, 145 (1995).
[15] H. Suzuki, Num. Astrophys. in Japan **2**, 267 (1991); in *Frontiers of Neutrino Astrophysics*, ed. by Y. Suzuki and K. Nakamura (Univ. Acad, Press, Tokyo, 1993), p. 219.
[16] J. A. Pons *et al.*, Astrophys. J. **513**, 780 (1999).
[17] S. Wanajo *et al.*, Astrophys. J. **695**, 208 (2009). A. J. T. Poelarends *et al.*, Astrophys. J. **675**, 614 (2008).
[18] F. S. Kitaura, H.-T. Janka and W. Hillebrandt, Astron. Astrophys. **450**, 345 (2006).
[19] H.-T. Janka *et al.*, Astron. Astrophys. **485**, 199 (2008).
[20] T. Fischer *et al.*, arXiv:0908.1871.
[21] K. Nomoto, Astrophys. J. **277**, 791 (1984); **322**, 206 (1987).
[22] H. Shen *et al.*, Nucl. Phys. A **637**, 435 (1998).
[23] M. Rampp and H.-T. Janka, Astron. Astrophys. **396**, 361 (2002).
[24] A. Marek *et al.*, Astron. Astrophys. **445**, 273 (2006).
[25] M. Liebendörfer *et al.*, Astrophys. J. **620**, 840 (2005)
[26] B. Müller, PhD Thesis (Techn. Univ. München 2009); B. Müller, H.-T. Janka, and H. Dimmelmeier, in prep.
[27] H. Dimmelmeier, J. A. Font and E. Müller, Astron. Astrophys. **388**, 917 (2002).
[28] R. Buras *et al.*, Astron. Astrophys. **447**, 1049 (2006).
[29] K. Langanke *et al.*, Phys. Rev. Lett. **90**, 241102 (2003). K. Langanke *et al.*, Phys. Rev. Lett. **100**, 011101 (2008).
[30] S. W. Bruenn, Astrophys. J. Suppl. **58**, 771 (1985).
[31] S. Reddy, M. Prakash and J. M. Lattimer, Phys. Rev. D **58**, 013009 (1998). S. Reddy *et al.*, Phys. Rev. C **59**, 2888 (1999). A. Burrows and R. F. Sawyer, Phys. Rev. C **58**, 554 (1998); **59**, 510 (1999).
[32] H.-T. Janka and W. Hillebrandt, Astron. Astrophys. **224**, 49 (1989).
[33] J. M. Lattimer and M. Prakash, Astrophys. J. **550**, 426 (2001).
[34] R. D. Hoffman, S. E. Woosley and Y.-Z. Qian, Astrophys. J. **482**, 951 (1997).
[35] B. Jegerlehner, F. Neubig and G. Raffelt, Phys. Rev. D **54**, 1194 (1996).
[36] R. Buras *et al.*, Astron. Astrophys. **457**, 281 (2006). L. Dessart *et al.*, Astrophys. J. **645**, 534 (2006).
[37] W. Keil, H.-T. Janka and E. Müller, Astrophys. J. **473**, L111 (1996).
[38] A. Arcones *et al.*, Phys. Rev. C **78**, 015806 (2008).